Computers and Chemical Engineering 146 (2021) 107217

Contents lists available at ScienceDirect

Computers and Chemical Engineering

journal homepage: www.elsevier.com/locate/compchemeng

Model predictive control for combined cycles integrated with CO_2 capture plants

Jairo Rúa[a,*], Magne Hillestad[b], Lars O. Nord[a]

[a] Department of Energy and Process Engineering, Norwegian University of Science and Technology, Norway
[b] Department of Chemical Engineering, Norwegian University of Science and Technology, Norway

ARTICLE INFO

Article history:
Received 14 September 2020
Revised 23 December 2020
Accepted 28 December 2020
Available online 31 December 2020

Keywords:
Gas turbine combined cycle
Amine absorption process
Monoethanolamine (MEA)
Dynamic modelling and simulation
Advanced control strategy
Post-combustion CO_2 capture

ABSTRACT

Flexible thermal power plants integrated with CO_2 capture systems can balance the intermittent power generation of renewable energy sources with low-carbon electricity. Among these power systems, natural gas combined cycles will play a fundamental role because of their faster operation and higher efficiency. Optimisation-based control strategies can enhance the flexible power dispatch of these systems and improve their performance during transient operation. This work proposes a model predictive control (MPC) strategy to stabilise these power plants with post-combustion CO_2 capture based on temperature swing chemical absorption and provide offset-free reference tracking. A delta-input formulation with disturbance modelling is proposed, as it provides more efficient computation with offset-free control. Data-based models were developed to replicate the performance of the actual power and capture plants. Prediction of nonlinear behaviour was accomplished by creating a network of local linear models, which allowed the formulation of the dynamic optimisation program in the MPC strategy as a convex quadratic programming problem. A case study demonstrated the effectiveness of the proposed MPC to balance drastic changes on power demand and keep specified capture ratios. Furthermore, the reduced deviations achieved in the reboiler temperature suggest that the nominal value of this parameter could be increased to improve the desorption process without risks of reaching temperatures where the solvent would degradate.

1. Introduction

Climate change mitigation requires a profound reduction of greenhouse gas emissions (IPCC, 2014; 2018). By sector, power generation is the main contributor to global CO_2 emissions because of its reliance on fossil fuels (IEA, 2019). Deployment of intermittent renewable energy sources, mainly wind and solar, has concentrated most of the efforts to decarbonise this sector (IEA, 2019). However, a broader portfolio of technologies is necessary to meet the increasing power demand whilst ensuring a safe, efficient and sustainable electric market. In this context, the integration of flexible carbon capture and storage (CCS) with thermal power plants is expected to play a fundamental role in the reduction of the CO_2 emissions associated with the power sector (IPCC, 2005; 2014).

Thermal power plants, especially natural gas combined cycles (NGCC), are recognised as a viable technology to accommodate the intermittent power generation from renewable energy sources and balance the electric grid (Kondziella and Bruckner, 2016; Eser et al., 2017; González-Salazar et al., 2017). Flexible CCS may enhance this dispatchable nature of flexible thermal power plants by providing low carbon electricity in a cost effective manner (Montañés et al., 2016; Heuberger et al., 2016; 2017a; 2017b). Post-combustion CO_2 capture (PCC) based on liquid-absorbents is arguably the most mature CCS technology, with two commercial-scale capture facilities integrated with coal power plants in operation (Bui et al., 2018). Nevertheless, the deployment of this technology in power markets dominated by intermittent renewable energy sources requires the demonstration that integration of CCS and thermal power plants does not inhibit flexible and efficient power generation, and stable CO_2 capture.

The dominant dynamics that govern the transient operation of thermal power plants, CO_2 capture plants and systems integrated by both technologies were extensively analysed by Rúa et al. (2020b). Two different dynamic behaviour define transient operation of these technologies. Thermal power plants operate in short time-scales and are limited by the large heat capacitance of the steam generator, whereas post-combustion CO_2 cap-

* Corresponding author.
E-mail addresses: jairo.r.pazos@ntnu.no (J. Rúa), lars.nord@ntnu.no (L.O. Nord).

https://doi.org/10.1016/j.compchemeng.2020.107217

Nomenclature

Latin Symbols

$\hat{A}$	State estimation
$\tilde{A}$	Delta-input state matrix
A	State matrix
$A(q^{-1})$	Polynomial ARX model
A_a	Augmented state matrix
a	Coefficients simplified models
$\tilde{B}$	Delta-input input matrix
B	Input matrix
$B(q^{-1})$	Polynomial ARX model
B_a	Augmented input matrix
B_d	Disturbance input matrix
b	Coefficients simplified models
$\tilde{C}$	Delta-input output matrix
C	Output matrix
c	Centre validity function
C_a	Augmented output matrix
C_d	Disturbance output matrix
Δu	Delta-input control vector
δu	Delta-input control action
d	Disturbance vector
F	MIMO delta-input penalty vector
f	Delta-input penalty vector
G	MIMO delta-input inequality matrix
g	Delta-input inequality matrix
H	Delta-input matrix output equation
I	Identity matrix
J	Objective function
K	Observer gain matrix
K_f	Kalman filter
M	number local ARX models
N	Time horizon
P	MIMO delta-input inequality vector
p	Delta-input inequality vector
Q	Weight matrix
q^{-1}	Backwards shift operator
Q_p	Process noise covariance
R	Penalty vector
R^2	Coefficient of determination
R_m	Measurement noise covariance
t	Time (s)
u	Manipulated variable
w	Width validity function
$\tilde{x}$	Delta-input state vector
x	State vector
x_a	Augmented input state vector
y	Predicted variable, output vector
Z	Estimator covariance matrix

Greek Symbols

Γ	Delta-input weight matrix
γ	Local operating point
λ	Weights objective function
Φ	MIMO delta-input weight matrix
Ψ	Unit lower triangular matrix
ξ	Local validity function
σ^2	Covariance
ε	Stochastic error

Subscripts

0	Initial conditions
d	Disturbance
n_u	Order ARX input
n_y	Order ARX output
pow	Power
ramp	Ramping rate
ref	Reference trajectory
u	Inputs
x	States

Superscripts

-	Previous estimation
low	Lower bound
up	Upper bound

ture plants are characterised by slow responses and long time-scales owing to the large volumes of stored solvent, the impact of large vessels on residence time, and the transport delay introduced by some equipment. This different transient behaviour does not limit power generation since variable steam extraction from the intermediate and low pressure cross-over of the steam turbine does not significantly affect the steam cycle of the power plant, albeit it has an impact on process variables of the CO_2 capture plant (Rúa et al., 2020b). Thus, control strategies must consider the different dynamic nature of thermal power plants and post-combustion CO_2 capture plants to adequately stabilise the process variable of each plant within their operation time-scales.

Control of traditional thermal power plants refers to matching the power generation to the demand and the stabilisation of the steam cycle. Natural gas combined cycles utilise the gas turbine to control power generation owing to their fast dynamics (Kehlhofer et al., 2009). Coal and biomass power plants must adapt the fuel and air injected in the boiler and throttle the superheated and reheated steam flow at the inlet of the steam turbine (Alobaid et al., 2017). Power generation control in coal and biomass power plants is hence dominated by the heat capacitance of the boiler. Therefore, the fast transient operation of gas turbines and their capability to adapt the power output within seconds make NGCCs more suitable for flexible operation and grid balance than coal and biomass power plants (Hentschel et al., 2016; Eser et al., 2017). Furthermore, NGCCs can under- and over-shoot the power generated by the gas turbine to compensate the slower transient of the steam cycle, enhancing the flexibility that this type of power plants provide to the grid (Rúa et al., 2020a; Rúa and Nord, 2020).

Steam cycle control includes the regulation of the fluid inventory in the steam drums, deaerators, condensers, and storage vessels; pressure control of the low-, medium- and high-pressure sections of the steam cycle; and temperature limitation of the superheated and reheated steam to avoid damaging the pipe system and the steam turbine. Inventory control refers to the stabilisation of the mass flows so the steady-state mass balances for each of the components and the overall power plant are satisfied (Aske and Skogestad, 2009). Proportional-integral (PI) controllers are normally used for control of water levels since the main objective of this control layer is to stabilise power plant operation, although three-element controllers where the drum level, feedwater flow and live-steam flow are embedded in a PID (proportional-integral-derivative) cascade controller are traditionally implemented in thermal power plants (Mansour et al., 2003; Kehlhofer et al., 2009). These controllers adjust the feedwater mass flow by changing the speed of the pumps or the opening of the control valves, depending on the type and design of the power plant. Model predictive control (MPC) strategies lead to further improvements in the inventory control of traditional power plants because of the dynamic optimisation carried out to determine the most suitable control action (Lu and Hogg, 1997; Prasad et al., 2000).

Pressure control is achieved by adjusting the feedwater mass flow rate and by valve throttling, specially in the lower-pressure sections of NGCCs where the pressure in the drum and deaerator may be controlled (Casella and Pretolani, 2006; Montañés et al., 2017c). In the high-pressure section of the steam cycle, strategies such partial arc and sliding pressure control lead to better part-load performance (Kehlhofer et al., 2009; Jonshagen and Genrup, 2010). Partial arc control regulates the steam admittance into the steam turbine with several valves in the stator of the first stage. In contrast, these valves are close to fully-open during sliding pressure operation to allow the variation of the high pressure and keep almost constant volumetric flow in the turbine, which results in higher part-load isentropic efficiency (Jonshagen and Genrup, 2010). If the high pressure of the steam cycle is not allowed to fluctuate, optimisation-based strategies lead to improved control of this pressure as they reduce the deviation from its set-point (Lu and Hogg, 1997; Prasad et al., 1998; 2000; Peng et al., 2009)

The temperature in the hot sections of the steam cycle, i.e. the outlet of the supeheater and reheater, must be controlled to avoid damaging the materials. Spray cooling is hence necessary to inject pressurised water in the steam flow and reduce its temperature. The opening of the attemperator valves regulating the flow of pressurised water may be defined by PID controllers (Alobaid et al., 2008; Kehlhofer et al., 2009; Montañés et al., 2017c; Garðarsdóttir et al., 2017), adaptative controllers (Matsumura et al., 1998), or optimisation-based controllers (Peng et al., 2009; Prasad et al., 1998, 2000; Rúa et al., 2020a; Rúa and Nord, 2020). Among the different alternatives to regulate the maximum temperature in the steam cycle, model predictive control shows the minimum offset from the set-point and the fastest stabilisation time (Rúa et al., 2020a; Rúa and Nord, 2020).

In contrast to thermal power plants, control of post-combustion CO_2 capture plants is not a mature field and most of the available knowledge comes from dynamic studies and test campaigns in pilot plants. Basic control of PCC plants reduces to stabilise liquid levels in sumps of absorber and stripper columns, reboiler and condenser; regulate the temperature of lean solvent and condenser; adapt the pressure of the reboiler and CO_2 product, and maintain a constant solvent composition (Panahi and Skogestad, 2011; Schach et al., 2013; Flø et al., 2015; 2016; Walters et al., 2016; Montañés et al., 2017a; 2018; Wu et al., 2020). Temperature control is achieved by heat exchangers where the mass flow rate of cooling water is the manipulated variable, whereas inventory control requires several pumps to stabilise liquid levels in different equipment, although valves may also be used. Throttling regulates the pressure of product of CO_2 and the mass flow rate of make-up solvent, or water, needed for a constant composition. Control of all these process variables may lead to over-constrained systems, and some might be left uncontrolled. For instance, the level in the reboiler is controlled and the sump level in the stripper varies freely in the Brindisi pilot plant (Flø et al., 2016), whereas the opposite inventory control approach is implemented at Technology Centre Mongstad (TCM) (Montañés et al., 2017a; 2018).

This basic control strategy aims at stabilising the main process variables and ensuring safe operation of PCC plants. Therefore, PID controllers are normally implemented. This control layer is similar among different pilot plants and dynamic process models (see e.g. the reviews by Salvinder et al. (2019) and Wu et al. (2020)). The main difference in control strategies and performance of PCC plants lies on the pairings and methods used to control performance indicators, i.e. capture rate or CO_2 product, liquid solvent to gas (L/G) ratios, energy performance ratios, and reboiler performance, where the latter may refer to outlet solvent temperature, outlet lean loading or heat duty. The majority of pairings between controlled and manipulated variables originate from insights obtained during process dynamic simulations, albeit relative gain array (RGA) analyses and self-optimisation procedures have been proposed (Panahi and Skogestad, 2011; 2012; Schach et al., 2013; Nittaya et al., 2014; Sahraei and Ricardez-Sandoval, 2014; Luu et al., 2015; Manaf et al., 2016; Gaspar et al., 2016). Different control design strategies may lead to distinct pairings with various performance, but none of the design methods have proved systematically superior.

Traditional PID controllers are able to reject disturbances and track references of CO_2 capture rates by modifying the mass flow rate of lean/rich solvent at the inlet/outlet of the absorber column (Lawal et al., 2010; Nittaya et al., 2014; Garðarsdóttir et al., 2015; Luu et al., 2015; Manaf et al., 2016; Gaspar et al., 2016; Montañés et al., 2017a), or the steam flow in the reboiler, i.e. the heat duty (Panahi and Skogestad, 2011; Nittaya et al., 2014; Montañés et al., 2017a). Similarly, PIDs can achieve close to contant reboiler temperature (Lawal et al., 2010; Panahi and Skogestad, 2011; 2012; Nittaya et al., 2014; Walters et al., 2016; Montañés et al., 2017a; 2018), L/G ratios (Garðarsdóttir et al., 2015; Montañés et al., 2017a; 2018), lean solvent loading (Garðarsdóttir et al., 2015; Gaspar et al., 2016) or energy performance indicators (Luu et al., 2015; Manaf et al., 2016) by manipulating the mass flow rate of solvent or the reboiler heat duty. These studies demonstrate PID controllers can stabilise PCC plants subjected to large disturbances within reasonable periods of time, albeit the lack of agreement on the most adequate pairing for key process variables.

Nevertheless, PID controllers may not be able to stabilise process variables within desirable bounds and can require excessively long settling times if the tuning is not adequate or the disturbance too drastic (Luu et al., 2015). Model predictive control can address these challenges by computing the control input through a dynamic optimisation problem where constraints in the controlled and manipulated variables ensure that process parameters remain within acceptable limits. MPC also originates less oscillations of smaller amplitude than PIDs for a given disturbance (Arce et al., 2012; Sahraei and Ricardez-Sandoval, 2014; Luu et al., 2015; Zhang et al., 2016; He et al., 2018; Li et al., 2018; Wu et al., 2018a; 2019a). This behaviour is due to the optimisation of predicted trajectories over a time horizon, which leads to shorter settling times and tighter control of PCC plants. Hauger et al. (2019) demonstrated the tight control achieved by MPC strategies in different tests performed in two pilot facilities (Tiller and TCM).

Furthermore, economic criteria such as market prices or energy cost may be included in MPC formulations to reduce the penalty of CCS systems while keeping PCC plants stable (Arce et al., 2012; Decardi-Nelson et al., 2018). This eases the integration of scheduling and control strategies since the outputs of the scheduling process may modify, in addition to the set-points of the controlled variables, tuning parameters in the optimisation problem included in the MPC (He et al., 2016).

Whilst there are several studies analysing control strategies for these different technologies operating independently, there are relative few studies considering the control of thermal power plants integrated with post-combustion CO_2 capture plants (Lawal et al., 2012; Mechleri et al., 2017; Garðarsdóttir et al., 2017; Montañés et al., 2017c; Marx-Schubach and Schmitz, 2019; Wu et al., 2019b; 2019c). Decentralised PID controllers can stabilise these integrated systems within their different time-scales, where the dominant dynamics of each plant dictate the settling time. However, the integration of CO_2 capture plants increases the settling time of process variables (e.g. steam pressure) in coal and natural gas thermal power plants because of the long stabilisation periods of CO_2 capture systems (Lawal et al., 2012; Garðarsdóttir et al., 2017; Montañés et al., 2017c; Mechleri et al., 2017). Similarly to control strategies in individual PCC plants, pairing of controlled and manipulated variables affects notably the performance of these decentralised controllers, as it influences the amplitude of fluctua-

tion and settling time of different process variables in both plants (Garðarsdóttir et al., 2017; Montañés et al., 2017c; Mechleri et al., 2017). Moreover, PID controllers can also regulate the start-up of integrated systems and achieve desirable CO_2 capture rates and power generation (Marx-Schubach and Schmitz, 2019).

Model predictive control can improve the control of thermal power plants integrated with CO_2 capture systems and reduce the settling time of key performance variables (Wu et al., 2019b; 2019c). MPC also enables the definition of different operation modes, which allows prioritising power generation, grid balancing or CO_2 capture according to market conditions and current regulations (Wu et al., 2019b; 2019c). However, power generation from coal-fired power plants is still limited by the heat capacitance of the steam generator, and MPC strategies can only enhance their flexible operation by reducing the steam extraction from the CO_2 capture plant, which leads to momentarily decreases of carbon capture (Wu et al., 2019b; 2019c). Natural gas combined cycles regulate their power generation through the gas turbine, and do not need to modify the steam extraction from the capture plant to balance the grid. Therefore, application of MPC strategies to NGCCs integrated with PCC plants can further enhance the flexible operation of both systems while taking advantage of the fast transient operation of NGCCs to balance power generation and demand.

This work demonstrates the application of model predictive control strategies to full-scale natural gas combined cycles integrated with post-combustion CO_2 capture plants with the objective of minimising the deviation of key process variables from their set-points. Section 2 describes the dynamic, full-scale NGCC-PCC model and the simplified models used in the MPC strategy, while Section 3 discusses how to achieve offset-free MPC with these simplified models and details its mathematical formulation. Section 4 demonstrates the fast control achieved by the proposed MPC strategy through a case study where the integrated system needs to balance a decrease in power demand. Final remarks and conclusions are included in Section 5.

2. Modelling

This section includes the different models developed to demonstrate the application of model predictive control strategies to natural gas combined cycles integrated with capture plants. Section 2.1 describes the high-fidelity model used to replicate the behaviour of the NGCC-PCC system, whereas Section 2.2 presents the simplified models included in the dynamic optimisation problem to predict the future behaviour of the actual system.

2.1. Dynamic modelling of a NGCC-PCC system

Natural gas combined cycles are expected to balance the intermittent power generation associated with renewable energy sources because of their fast and flexible operation. Moreover, triple-pressure NGCCs with reheating are the most efficient and less polluting fossil-fuelled thermal power plants (Kehlhofer et al., 2009; Alobaid et al., 2017). This study considers a full-scale 615 MWe NGCC with this configuration. The design was carried out with GT PRO (Thermoflow, 2014) because it provides detailed descriptions of the geometry of the equipment, off-design performance, and operation maps of pumps and gas turbines. This data was implemented in a high-fidelity dynamic model developed in Modelica (Modelica Association, 2019; Dassault Systemes, 2016) with the specialized TPL library (Modelon, 2015), which is based on conservation equations, detailed heat transfer and pressure drop correlations, and maps of performance for the turbomachinery components.

This thermal power plant was integrated with a full-scale 30 wt% MEA-based post-combustion capture process, as this is the most mature CCS technology available. System integration occurred between the intermediate- and low-pressure steam turbines of the NGCC and the reboiler of the PCC plant, where steam extracted from the steam cycle provides the energy to regenerate the solvent in the capture plant. The design of the low-pressure section of the steam turbine was adapted to nominal operating conditions, i.e. steam is extracted to achieve a 90% capture rate at 100% gas turbine load (Jordal et al., 2012; Rezazadeh et al., 2015). Furthermore, the design of the PCC plant considered the nominal CO_2 capture rate, the exhaust gas CO_2 concentration and conditions (i.e. flow rate, temperature, pressure), the allowable pressure drops in the absorber and stripper columns, column flooding limits and a reasonable balance between capital and operational costs (Jordal et al., 2012; Dutta et al., 2017). Because of the size of the NGCC and the amount of flue gas generated, these requirements were met with a parallel configuration with two absorber columns and one stripper (Montañés et al., 2017c; Dutta et al., 2017). A detailed modelling description and thorough validation results of these dynamic models can be found in the work by Montañés et al. (2017c). Fig. 1 represents the layout of the NGCC-PCC system.

These plants exhibit different dynamic behaviour. Load changes in the gas turbine lead to immediate variations in the exhaust gas conditions. However, these changes affect progressively the steam cycle. Thus, the heat capacitance of the HRSG dominates the transient performance of the NGCC. For thermal power plants of this type and size, step changes in the exhaust gas conditions show dominant dynamics of approximately 10 min, with stabilisation times of 20–25 min (Hentschel et al., 2016; Montañés et al., 2017c). PCC plants have slower transient performance because of the long residence time of the solvent, the transport delay introduced by heat exchangers, and the large amount of solvent stored in vessels and liquid hold-ups (Rúa et al., 2020b). Similarly, step changes in the exhaust gas conditions show that the dominant dynamics of PCC plants of this size occur in approximately 60 min with stabilisation times of several hours (Lawal et al., 2010; 2012; Flø et al., 2015; 2016; Garðarsdóttir et al., 2015; Montañés et al., 2017c; 2017b).

2.2. System Identification

The computational cost of simulating the high-fidelity dynamic model of the NGCC-PCC system described in Section 2.1 inhibits its utilisation in optimisation-based control strategies. Therefore, simplified models that replicate the behaviour of specific thermodynamic variables (e.g. reboiler temperature, capture rate, mechanical power generation) are required to predict the performance of the integrated system in the model predictive control strategy proposed in this work.

System identification refers to the development of data-based dynamic models (Ljung, 1987), and was utilised to develop autoregressive models with exogenous variables (ARX) that predict the dynamic behaviour of variables of interest. Eq. (1) represents the general structure of an ARX model:

$$A(q^{-1})\,y(t) = B(q^{-1})\,u(t) + \varepsilon(t) \tag{1}$$

where y is the predicted and controlled variable, u is the manipulated variable associated with it, A and B are polynomials in the backwards shift operator q^{-1} of order n_y and n_u, respectively, and $\varepsilon \in \mathcal{N}(0, \sigma^2)$.

$$A(q^{-1}) = 1 + a_1\,q^{-1} + a_2\,q^{-2} + \cdots + a_{n_y}\,q^{-n_y}$$

$$B(q^{-1}) = b_1\,q^{-1} + b_2\,q^{-2} + \cdots + b_{n_u}\,q^{-n_u}$$

Table 1 summarises the set of input-output pairs, i.e. the controlled variable and its associated manipulated variable, considered in this work to control the operation of the NGCC-PCC system. These input-output pairs present nonlinear behaviour and

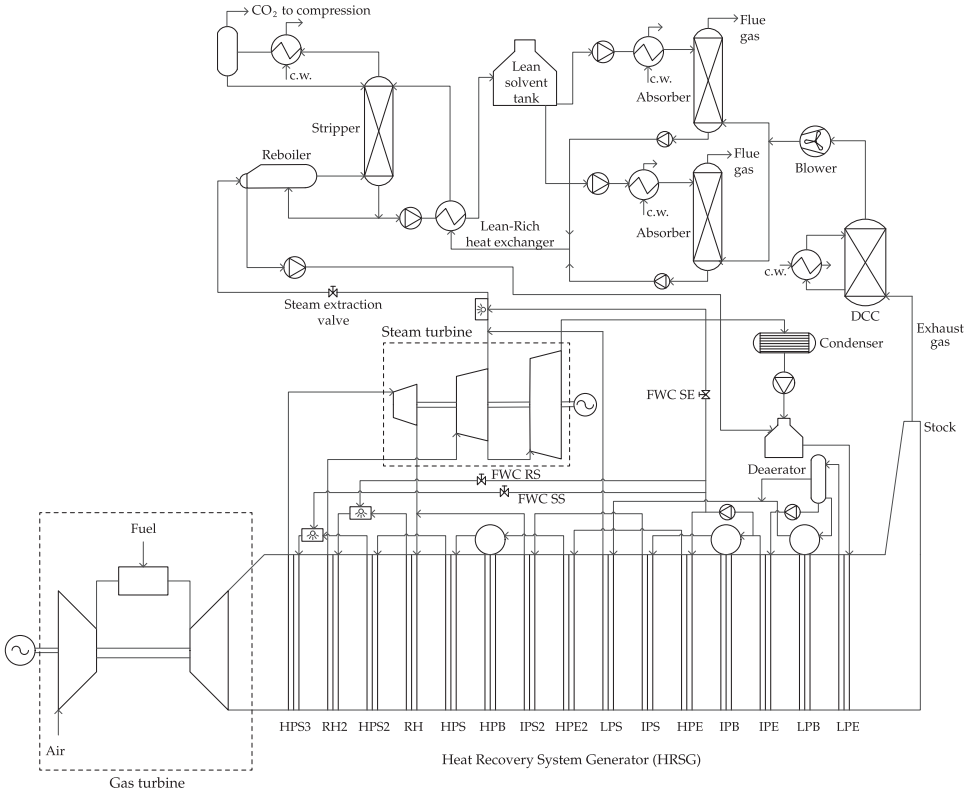

Fig. 1. Process diagram of the natural gas combined cycle integrated with the post-combustion capture plant.The nomenclature is as follows. E: Economiser, B: Boiler, S: Superheater, R: Reheater P: Pressure, L: Low, I: Intermediate, H: High, FWC: Feed-water cooling, RS: Reheated steam, SS: Superheated steam, SE: steam extraction, DCC: Direct contact cooler, c.w.: cooling water.

single ARX models cannot predict them accurately in broad operation ranges because of their linearity. Local model networks of linear ARX models can overcome this limitation (Johansen and Foss, 1993; Wu et al., 2018b; Jung et al., 2020). This modelling approach relies on the development of several linear ARX models at different operation points for each input-output pair. The overall prediction of a local model network is the result of interpolating the individual predictions of the local ARX models according to current operation point (Johansen and Foss, 1993). Thus, local models neighbouring this operation condition contribute more to the overall prediction than locals models of regimes far from the operation point. The output of a local model network is:

$$y(t) = \sum_{i=1}^{M} y_i(t)\ \xi_i(\gamma) \tag{2}$$

where M is the number of local models for each input-output pair, $y_i(t)$ represents the outputs of the local ARX models, ξ is the local validity function that weights the contribution of each local ARX model, and γ is the parameter defining the current operating point. This is equivalent to first interpolating the parameters (a, b) of the local ARX models using the local validity function ξ and then computing the output of the overall ARX model with these parameters.

This work considered a Gaussian validity function because it satisfies a necessary condition to achieve arbitrarily good predictions with local model networks (Johansen and Foss, 1993):

$$\xi_i(\gamma) = \frac{\exp\left(-\frac{1}{2}[(\gamma - c_i)/w_i]^2\right)}{\sum_{j=1}^{M} \exp\left(-\frac{1}{2}\left[\left(\gamma - c_j\right)/w_j\right]^2\right)} \tag{3}$$

where c_i and w_i are, respectively, the centres and widths of the local Gaussian interpolation functions. Table A.4 includes the number of local models for each input-output pair, the parameters of each local ARX model, and the variables defining their validity functions.

Data to generate these models was obtained from excitation of the high-fidelity model described in Section 2.1 at different operation conditions. Therefore, each set of data was used to generate a single local ARX model for every input-output pair. Random gaussian signals (RGS) were superimposed on the controllers of the NGCC-PCC system in closed-loop since this approach enhances the identification of ARX models (Gevers and Ljung, 1986; Forssell and Ljung, 1999; Gevers, 2005; Gevers et al., 2006; Mišković et al., 2008). In addition, an unique validation set of data covering the entire operation range of the NGCC-PCC system was generated following the same approach.

Table 1 summarises the prediction accuracy of the local model network for each input-output pair measured by the coefficient of determination R^2. The low R^2 of the simplified models for the superheating and reheating temperature originate from the nature of the validation data. The RGS signals superimposed on the controllers to generate the identification data fluctuated faster than the dominant dynamics of the steam cycle, which lead to drastic and fast changes in the controlled and manipulated variables of the NGCC. This created a challenging set of data that allowed testing whether the local model network could predict large and frequent fluctuations. In contrast, the PCC data does not show this behaviour because of the slower dominant dynamics of the capture plant and its buffering effect, mainly through solvent vessels and liquid hold-ups (Rúa et al., 2020b). This transient performance results in smoother and slower variations easier to predict that lead to higher R^2 values. Fig. B.4 illustrates this different behaviour between the NGCC and PCC plants for a small set of the validation data, and how the ARX models of the NGCC adequately predict the trajectory of the output variables despite the lower R^2 values.

Table 1
Input-output pairs with model order and coefficient of determination.

Plant	Input-output pair		Order		Nominal		R^2[%]
	Controlled variable (y)	Manipulated variable (u)	n_y	n_u	n_y	n_u	
NGCC	Power generation	Gas turbine load					99.95
	Superheated steam temperature	Opening attemperator valve 1	2	2	592.7 °C	0.02655	69.59
	Reheated steam temperature	Opening attemperator valve 2	2	2	592.5 °C	0.07882	74.37
PCC	Capture rate	Mass flow lean solvent	1	1	90 %	614	98.40
	Reboiler temperature	Opening steam extraction valve	1	1	119.22 °C	0.69	99.09

In contrast to the other simplified models, the power generation of the NGCC was predicted using an unique polynomial over the entire set of operating conditions. A simple representation for this variable is possible owing to the linear relationship between the power generation of the NGCC and the load of the gas turbine over a broad operating region. The structure of this model is:

$$y(t) = a + b\,u(t) \tag{4}$$

ARX models are suitable for system identification procedures because the computation of their coefficients becomes a simple least-square problem or a convex optimisation, whereas other structures may involve more complex, possibly non-convex, identification problems (Huusom et al., 2010). However, for analysis purposes, state-space forms of ARX models are preferred. The realisation in observable form of the ARX model in Eq. (1) is:

$$x_{k+1} = A\,x_k + B\,u_k \tag{5a}$$

$$y_k = C\,x_k \tag{5b}$$

with

$$A = \begin{bmatrix} -a_1 & 1 & 0 & \cdots & 0 \\ -a_2 & 0 & 1 & \cdots & 0 \\ \vdots & \vdots & \vdots & \ddots & \vdots \\ -a_{n_y-1} & 0 & 0 & \cdots & 1 \\ -a_{n_y} & 0 & 0 & \cdots & 0 \end{bmatrix} \quad B = \begin{bmatrix} 0 \\ \vdots \\ b_1 \\ \vdots \\ b_{n_u} \end{bmatrix} \quad C = [1\,0\,\cdots\,0]$$

where B has $n_y - n_u$ zeros, and $x \in \mathbb{R}^{n_y}$, $u, y \in \mathbb{R}$, $A \in \mathbb{R}^{n_y \text{x} n_y}$, $B \in \mathbb{R}^{n_y \text{x} 1}$, and $C \in \mathbb{R}^{1 \text{x} n_y}$. This realisation is valid when the ARX model leads to proper rational transfer functions, i.e. $n_y \geq n_u$. The stochastic error term in Eq. (1) is not included because of the deterministic data used during system identification.

3. Model predictive control

Control strategies based on MPC formulations require the development of different models and optimisation problems to ensure optimal computation of control inputs, offset-free tracking of controlled variables and adequate estimation of states. Fig. 2 shows a diagram of the MPC strategy proposed in this work. The high-fidelity dynamic model of the NGCC-PCC system described in Section 2.1 replicates the behaviour of a real power plant with post-combustion CO_2 capture. Measurements from this model allow the estimation of the states in the system. This estimator uses a Kalman filter to update the state estimations and correct possible mismatches between the predictions of the responses by the simplified models and the measurements from the dynamic simulation of the NGCC-PCC plant. These estimates define the current state, i.e. the initial conditions, from where the dynamic optimisation problem in the MPC strategy starts to compute the optimal sequence of control inputs. The first element of this sequence is the control action imposed in the actual system. This process is repeated periodically, with a frequency dictated by the sampling time, to stabilise the operation of the NGCC integrated with the

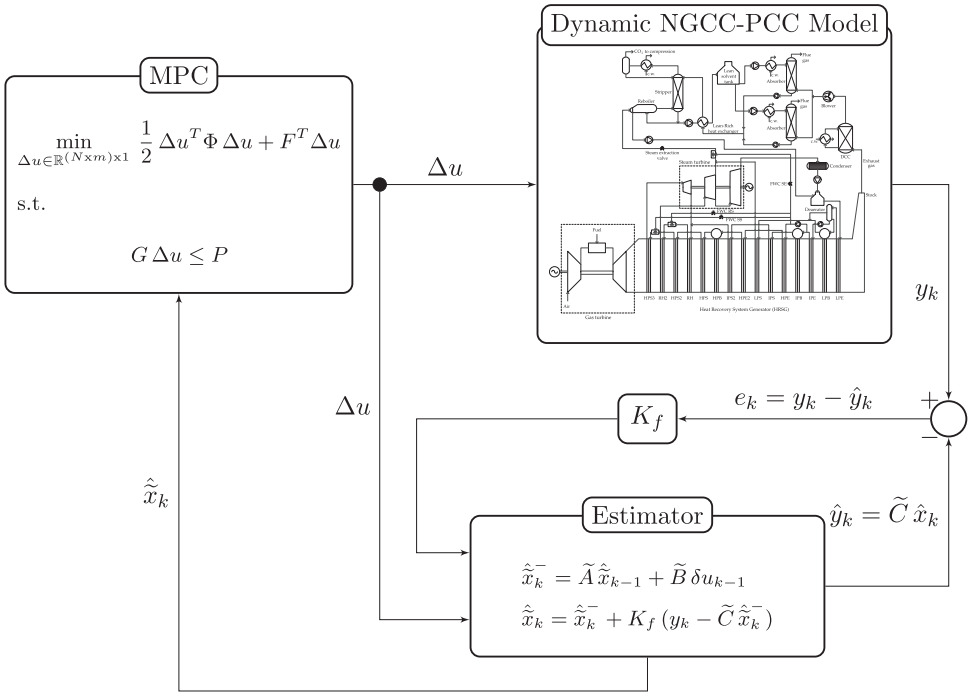

Fig. 2. Diagram of the proposed MPC strategy with a Kalman filter. Expressions within the diagram are developed throughout Section 3, while the dynamic model of the NGCC-PCC system is described in Section 2.1.

PCC plant. This MPC strategy includes all simplified models in a single controller as shown in Fig. 2.

This section describes different models and formulations of the MPC strategy, and details how they are combined in the integrated control structure represented in Fig. 2. Section 3.1 discusses reference tracking and offset-free MPC, and describes the formulation of this optimisation problem, whereas Section 3.2 builds up on this formulation and defines a simpler dynamic optimisation problem, called delta-input formulation, that only depends on the manipulated variables. Section 3.3 describes the estimator that predicts the states on the actual NGCC-PCC systems and presents an algorithm to solve the MPC control problem.

3.1. Reference tracking and offset-free MPC

Reference tracking is one of the main applications of model predictive control. This control strategy minimises the difference between outputs of a system and reference trajectories by computing control inputs through dynamic optimisation problems and implementing the first element of the calculated control sequence. The general formulation of linear MPC problems for reference tracking is:

$$\min_{x,u} \sum_{k=0}^{N-1} \frac{1}{2} \left\| Q\left(y_k - y_{\text{ref}}\right) \right\| + \left\| R\left(u_k - u_{k-1}\right) \right\| \tag{6a}$$

s.t.

$$x_{k+1} = A\,x_k + B\,u_k \tag{6b}$$

$$y_k = C\,x_k \tag{6c}$$

$$y^{\text{low}} \leq y_k \leq y^{\text{up}} \tag{6d}$$

$$u^{\text{low}} \leq u_k \leq u^{\text{up}} \tag{6e}$$

where $\|\cdot\|$ represents the two-norm that leads to a quadratic programming (QP) optimisation problem. Eq. (6b) and (6c) ensure that the state-space realisation of the identified ARX models is satisfied. Eqs. (6d) and (6e) limit the minimum and maximum values of the controlled and manipulated variables, respectively. The objective function in Eq. (6a) minimises the difference between controlled variables and their references y_{ref} and imposes a penalty in excessive utilisation of control inputs.

Nevertheless, reference tracking formulations of MPC strategies as in Eq. (6) can lead to offsets in the controlled variables due to unmeasured disturbances and plant-model mismatches. To overcome this limitation and ensure zero offset, models representing actual systems can be augmented with a disturbance model, which acts as an integrator driving the tracking error to zero. This allows finding the control inputs that minimise both the effect of the disturbance on the controlled variables and differences between model and system (Pannocchia and Rawlings, 2003; Borrelli and Morari, 2007; Pannocchia, 2015; Rawlings et al., 2017). The state-space model in Eq. (5) becomes:

$$x_{\text{a},k+1} = A_{\text{a}}\,x_{\text{a},k} + B_{\text{a}}\,u_k \tag{7a}$$

$$y_k = C_{\text{a}}\,x_{\text{a},k} \tag{7b}$$

where vectors and matrices are:

$$\begin{bmatrix} x_{k+1} \\ d_{k+1} \end{bmatrix} = \begin{bmatrix} A & B_{\text{d}} \\ 0 & I \end{bmatrix} \begin{bmatrix} x_k \\ d_k \end{bmatrix} + \begin{bmatrix} B \\ 0 \end{bmatrix} u_k$$

$$y_k = \begin{bmatrix} C & C_{\text{d}} \end{bmatrix} \begin{bmatrix} x_k \\ d_k \end{bmatrix}$$

This augmented model achieves offset-free tracking if the system is stabilisable, the pair (A, C) is observable, the number of disturbances n_{d}:

$$n_{\text{d}} = p = 1$$

and the following condition holds (Pannocchia and Rawlings, 2003; Borrelli and Morari, 2007; Pannocchia, 2015; Rawlings et al., 2017):

$$\text{rank}\begin{bmatrix} A - I & B_{\text{d}} \\ C & C_{\text{d}} \end{bmatrix} = n_y + n_{\text{d}}$$

Since the disturbance matrices $B_{\text{d}} \in \mathbb{R}^{n_y x n_{\text{d}}}$ and $C_{\text{d}} \in \mathbb{R}^{1 x n_{\text{d}}}$ can be chosen freely, the last condition holds if (A, C) is observable. In this work, the state-space realisation of the identified ARX models was expressed in observable form, and hence the pair (A, C) is always observable (Chen, 2013). Therefore, offset-free tracking reduces to the adequate selection of disturbance matrices B_{d} and C_{d}.

The MPC formulation in Eq. (6) for the system augmented with a disturbance model becomes:

$$\min_{x,u} \sum_{k=0}^{N-1} \frac{1}{2} \left\| Q\left(y_k - y_{\text{ref}}\right) \right\| + \left\| R\left(u_k - u_{k-1}\right) \right\| \tag{8a}$$

s.t.

$$x_{\text{a},k+1} = A_{\text{a}}\,x_{\text{a},k} + B_{\text{a}}\,u_k \tag{8b}$$

$$y_k = C_{\text{a}}\,x_{\text{a},k} \tag{8c}$$

$$y^{\text{low}} \leq y_k \leq y^{\text{up}} \tag{8d}$$

$$u^{\text{low}} \leq u_k \leq u^{\text{up}} \tag{8e}$$

3.2. Delta-input formulation

Delta-input formulations of the MPC described in Eq. (8) are more suitable for reference tracking problems, as they penalise directly the rate of change of the manipulated variables (Borrelli and Morari, 2007). Furthermore, it reduces the number of optimisation variables and the computational cost of the dynamic optimisation. Section 3.2.1 describes the delta-input formulation of the MPC problem in Eq. (8), whereas Section 3.2.2 discusses how several state-space models can be merged into a common MPC problem.

3.2.1. Delta-input formulation for SISO systems

Define the delta-input control action that determines the rate of change of a manipulated variable:

$$\delta u_k := u_k - u_{k-1} \tag{9}$$

and augment the state-space equation in Eq. (7) with this new state and control input:

$$\begin{bmatrix} x_{\text{a},k+1} \\ u_k \end{bmatrix} = \begin{bmatrix} A_{\text{a}} & B_{\text{a}} \\ 0 & I \end{bmatrix} \begin{bmatrix} x_{\text{a},k} \\ u_{k-1} \end{bmatrix} + \begin{bmatrix} B_{\text{a}} \\ I \end{bmatrix} \delta u_k \tag{10a}$$

$$y_k = \begin{bmatrix} C_{\text{a}} & 0 \end{bmatrix} \begin{bmatrix} x_{\text{a},k} \\ u_{k-1} \end{bmatrix} \tag{10b}$$

which can be written:

$$\widetilde{x}_{k+1} = \widetilde{A}\,\widetilde{x}_k + \widetilde{B}\,\delta u_k$$

$$y_k = \widetilde{C}\,\widetilde{x}_k$$

Define the vectors of controlled and manipulated variables over a time horizon N:

$$\delta u = [\delta u_0 \ \delta u_1 \ \dots \ \delta u_{N-1}]^T$$

$$y = [y_1 \ y_2 \ \dots \ y_N]^T$$

and eliminate the states in Eq. (10). The output equation, over the time horizon N, becomes:

$$y = H\delta u + A_0\tilde{x}_0 \tag{11}$$

where

$$H = \begin{bmatrix} H_1 & 0 & \cdots & \cdots & 0 \\ H_2 & H_1 & 0 & \cdots & 0 \\ \vdots & \ddots & \ddots & \ddots & \vdots \\ \vdots & & H_2 & H_1 & 0 \\ H_N & \cdots & \cdots & H_2 & H_1 \end{bmatrix} \quad A_0 = \begin{bmatrix} \tilde{C}\tilde{A} \\ \tilde{C}\tilde{A}^2 \\ \tilde{C}\tilde{A}^3 \\ \vdots \\ \tilde{C}\tilde{A}^N \end{bmatrix}$$

with

$$H_i = \tilde{C}\tilde{A}^{i-1}\tilde{B} \qquad i \in \{1, 2, \dots, N\}$$

$$\tilde{x}_0 = \tilde{x}[0]$$

With this reduced output equation, Eq. (11), and the definition of the delta control input in Eq. (9), the inequality constraints in the standard MPC formulation, Eq. (8d) and Eq. (8e), can be written as:

$$\begin{bmatrix} -H \\ H \\ -\Psi \\ \Psi \end{bmatrix} \delta u \leq \begin{bmatrix} -(y^{\text{low}} - A_0\tilde{x}_0) \\ y^{\text{up}} - A_0\tilde{x}_0 \\ -(u^{\text{low}} - u_{-1}) \\ u^{\text{up}} - u_{-1} \end{bmatrix} \tag{12}$$

where u_{-1} was the control action in the previous sampling time, and Ψ is an unit lower triangular matrix:

$$\Psi = \begin{bmatrix} 1 & 0 & \cdots & \cdots & 0 \\ 1 & 1 & \ddots & & \vdots \\ \vdots & \ddots & \ddots & \ddots & \vdots \\ \vdots & & \ddots & 1 & 0 \\ 1 & \cdots & \cdots & 1 & 1 \end{bmatrix}$$

Following the same approach, the objective function Eq. (8a) becomes:

$$\begin{aligned} J &= \frac{1}{2}(\|Q(y - y_{\text{ref}})\| + \|R\delta u\|) \\ &= \frac{1}{2}(\|Q(H\delta u + A_0\tilde{x}_0 - y_{\text{ref}})\| + \|R\delta u\|) \\ &= \frac{1}{2}\big[\delta u^T\big(H^TQH + R\big)\delta u \\ &\quad + 2(A_0\tilde{x}_0 - y_{\text{ref}})QH\delta u \\ &\quad + (A_0\tilde{x}_0 - y_{\text{ref}})^TQ(A_0\tilde{x}_0 - y_{\text{ref}})\big] \end{aligned} \tag{13}$$

where the last term may be dropped since is constant.

Therefore, the MPC strategy can be expressed as the QP problem:

$$\min_{\delta u \in \mathbb{R}^N} \ \frac{1}{2}\delta u^T\Gamma\,\delta u + f^T\delta u \tag{14a}$$

s.t.

$$g\,\delta u \leq p \tag{14b}$$

with the matrix and vector in Eq. (14b) defined in Eq. (12), and:

$$\Gamma = H^TQH + R$$
$$f = (A_0\tilde{x}_0 - y_{\text{ref}})QH$$

The development of the MPC delta-input formulation for the polynomial model in Eq. (4) follows the same approach and is summarized in Appendix C.

3.2.2. Delta-input formulation for MIMO systems

Systems generally require the control of several process variables. Thus, the delta-input formulation of the MPC problem in Eq. (14) is expanded to consider multi-input multi-output (MIMO) systems. Consider m single-input single-output (SISO) models with manipulated variables defined as delta-input control actions and grouped in a vector as:

$$\Delta u := [\delta u_1 \ \delta u_2 \ \dots \ \delta u_m]^T \tag{15}$$

where each component is a sequence of control actions over a time horizon N for a given manipulated variable:

$$\delta u_j = [\delta u_{j,1} \ \dots \ \delta u_{j,N}]^T \qquad j \in \{1, \dots, m\}$$

The MPC delta-input formulation can be extended as:

$$\min_{\Delta u \in \mathbb{R}^{(Nxm)x1}} \ \frac{1}{2}\Delta u^T\Phi\,\Delta u + F^T\Delta u \tag{16a}$$

s.t.

$$G\Delta u \leq P \tag{16b}$$

where

$$\Phi = \begin{bmatrix} \Gamma_1 & 0 & \cdots & 0 \\ 0 & \Gamma_2 & \ddots & \vdots \\ \vdots & \ddots & \ddots & 0 \\ 0 & \cdots & 0 & \Gamma_m \end{bmatrix} \quad F = \begin{bmatrix} f_1 \\ f_2 \\ \vdots \\ f_m \end{bmatrix}$$

$$G = \begin{bmatrix} g_1 & 0 & \cdots & 0 \\ 0 & g_2 & \ddots & \vdots \\ \vdots & \ddots & \ddots & 0 \\ 0 & \cdots & 0 & g_m \end{bmatrix} \quad P = \begin{bmatrix} p_1 \\ p_2 \\ \vdots \\ p_m \end{bmatrix}$$

3.3. Estimator

States and disturbances need to be estimated from the measurements of the actual system at each sampling time to obtain the current state of the NGCC-PCC plant. The estimator, or observer, computes the augmented state at each discrete time k as a combination of the current, or a priori, state prediction and a correction based on the measured output y_k:

$$\hat{\tilde{x}}_k = \tilde{A}\hat{\tilde{x}}_{k-1} + \tilde{B}\,\delta u_{k-1} + K\,(y_k - \tilde{C}\,(\tilde{A}\hat{\tilde{x}}_{k-1} + \tilde{B}\,\delta u_{k-1})) \tag{17}$$

where $\hat{\cdot}$ indicates estimated variables, and $K \in \mathbb{R}^{(n_y+n_d+1)\,x\,1}$ is the observer gain:

$$K := \begin{bmatrix} K_x \\ K_d \\ K_u \end{bmatrix}$$

in which K_x, K_d, K_u are the observer gains for the states, disturbances and control input, respectively. This observer gain K is chosen so the observer is stable, i.e. the eigenvalues of the system $(\tilde{A} - K\tilde{C}\tilde{A})$ lie inside the unit circle.

Pole placement routines compute observer gain matrices that fix the eigenvalues of a matrix pair in specific coordinates and make the estimator stable (see, e.g. Pannocchia, 2015). However, this work considers a Kalman filter as observer gain matrix (Kalman, 1960). Calculation of the Kalman filter matrix gain is a two-step process. First, the a priori state $\hat{\tilde{x}}_{k-1}^-$ and covariance matrix Z_k^- are computed from previous estimations:

$$\hat{\tilde{x}}_k^- = \tilde{A}\hat{\tilde{x}}_{k-1} + \tilde{B}\,\delta u_{k-1} \tag{18a}$$

$$Z_k^- = \tilde{A}Z_{k-1}\tilde{A}^T + Q_p \tag{18b}$$

Algorithm 1 MPC for NGCC-PCC systems

Require: coefficients (a, b) in Table~A.4, B_d, C_d, Q_p, R_m, Q, R, y_{ref}, y^{low}, y^{up}, u^{low}, u^{up}, GT_{ramp}, Ψ, N

Require: $\hat{\tilde{x}}_{k-1}$, Δu_{k-1}, y_k, $\dot{m}_{exhaust}$, Z_{k-1}

Compute: interpolated coefficients (a, b) with Eqs.~2, 3

Compute: $\tilde{A}$, $\tilde{B}$, $\tilde{C}$ in Eq.~10

Compute: H, A_0 in Eq.~11

Compute: $\hat{\tilde{x}}_k$, Z_k in Eq.~18

Set: $\tilde{x}_0 := \hat{\tilde{x}}_k$

Compute: g, p in Eq.~12

Compute: Γ, f in Eq.~14a

Compute: G, P, Φ, F in Eq.~16

Solve:

$$\min_{\Delta u \in \mathbb{R}^{(Nxm)x1}} \frac{1}{2}\Delta u^T \Phi \Delta u + F^T \Delta u$$

s.t.

$$G\Delta u \leq P$$

return Δu_k, $\hat{\tilde{x}}_k$, P_k

with Q_p representing the covariance of the process noise $w \in \mathcal{N}(0, Q_p)$. Then, these a priori estimates are updated based on current measurements:

$$K_f = \frac{Z_k^- \tilde{C}^T}{\tilde{C} Z_k^- \tilde{C}^T + R_m} \tag{18c}$$

$$\hat{\tilde{x}}_k = \tilde{\hat{x}}_k^- + K_f (y_k - \tilde{C}\tilde{\hat{x}}_k^-) \tag{18d}$$

$$Z_k = (I - K_f \tilde{C}) Z_k^- \tag{18e}$$

where R_m is the covariance associated to the measurement noise $v \in \mathcal{N}(0, R_m)$, and K_f is the Kalman filter used to estimate the current state $\hat{\tilde{x}}_k$ and the covariance matrix Z_k that will be used at the next sampling time.

Algorithm 1 summarises the sequence of computations needed to implement the MPC strategy at each sampling time. The first require condition refers to the parameters, matrices and vectors provided off-line, whilst the second require condition indicates the parameters that are updated every sampling time. The mass flow rate of exhaust gas $\dot{m}_{exhaust}$ belongs to this second group as it is the parameter needed to interpolate the coefficients of the local ARX models for the capture ratio and reboiler steam temperature (see Table A.4). Moreover, note that the first element of each input control sequence must be selected from Δu_k.

4. Dynamic operation of NGCC-PCC integrated systems

A case study where the NGCC-PCC system needs to reduce its power generation to balance the grid demonstrates the effectiveness of the proposed MPC strategy to respond to fast changes in power demand and stabilise the operation of the integrated plants. The dominant dynamics of the NGCC and PCC described in Section 2.1 occur within 10 and 60 min, respectively. Thus, the MPC strategy considered a sampling time of 30 s in order to capture the transient behaviour in the shortest time-scale, i.e. the dynamic operation of the NGCC. A time horizon $N = 20$ was hence selected to consider the entire period of dominant dynamics in the NGCC. Table 2 includes the bounds for the controlled and manipulated variables considered during the dynamic simulations. Table 3 summarises the matrices and vectors to create the augmented models, the estimator based on the Kalman filter, and the weights in the objective function for each input-output pair. These

Table 2
Lower and upper bounds of the controlled and manipulated variables.

Variable	Lower	Upper
Power [MW]	450	615
Gas turbine load [%]	60	100
Superheating temperature [°C]	587.7	597.7
Attemperator valve 1 [-]	0.01	1
Reheating temperature [°C]	587.5	597.5
Attemperator valve 2 [-]	0.01	1
Capture ratio [-]	0.85	0.95
Mass flow lean solvent [kg/s]	300	800
Reboiler temperature [°C]	115.22	120.22
Steam extraction valve [-]	0.01	1

Table 3
Matrices and vectors defining the disturbance (B_d, C_d) and noise (Q_p, R_m) models; and weights for controlled variables (λ_Q) and penalties in movement of manipulated variables (λ_R).

Variable	B_d	C_d	Q_p	R_m	λ_Q	λ_R
Power	-	-	-	-	1	1
Superheating temperature	$\begin{bmatrix}0\\0\\0.01\end{bmatrix}$	0	I_{4x4}	0.01	10	0.01
Reheating temperature	$\begin{bmatrix}0\\0\\0.01\end{bmatrix}$	0	I_{4x4}	0.01	10	0.01
Capture ratio	$\begin{bmatrix}0.1\\0.1\end{bmatrix}$	0	I_{3x3}	0.1	50000	0.001
Reboiler temperature	$\begin{bmatrix}0.01\\0.01\end{bmatrix}$	0	I_{3x3}	0.1	100	10

weights aimed at compensating the different orders of magnitude between controlled and manipulated variables and at prioritising the tracking of the process variables, albeit their tuning was outside of the scope of this work.

A step change in the power demand drives the transient operation of the power plant, which adapts the gas turbine load to adjust the net power output. Similarly, the change in exhaust gas conditions disturbs the operation of the capture plant. Fig. 3 shows key process variables in the NGCC-PCC system during dynamic operation and demonstrates the effectiveness of the proposed MPC strategy to achieve optimal offset-free control.

Process variables from the NGCC reach their set-point faster because of the shorter dominant dynamics of the power plant compared to the capture system. Net power generation is the fastest variable to meet its target owing to the fast dynamics of the gas turbine, which controls the overall power output of the NGCC and compensates the slow dynamics of the steam cycle. Consequently, power demand and supply are balanced within the dominant dynamics of the NGCC. Temperature control in the superheating and reheating sections of the HRSG requires more time. Heat capacitance in the HRSG slows down the transient performance of the steam cycle compared to the change in gas turbine load. The attemperator valves need to compensate and anticipate these variations in the operating conditions for a longer period of time. Nevertheless, the proposed MPC strategy limited the offset and drove both temperatures to their set-point.

Dynamics in the PCC plant are notably slower than in any type of thermal power plant (Rúa et al., 2020a). However, Fig. 3 illustrates how the MPC strategy controlled the capture ratio almost simultaneously to the temperature in the steam cycle of the NGCC. This behaviour originates from the use of optimisation-based control strategies. MPC considers the dynamic operation of the capture plant and computes optimal control actions that achieved better and faster offset free in key process variables. Fig. 3 also il-

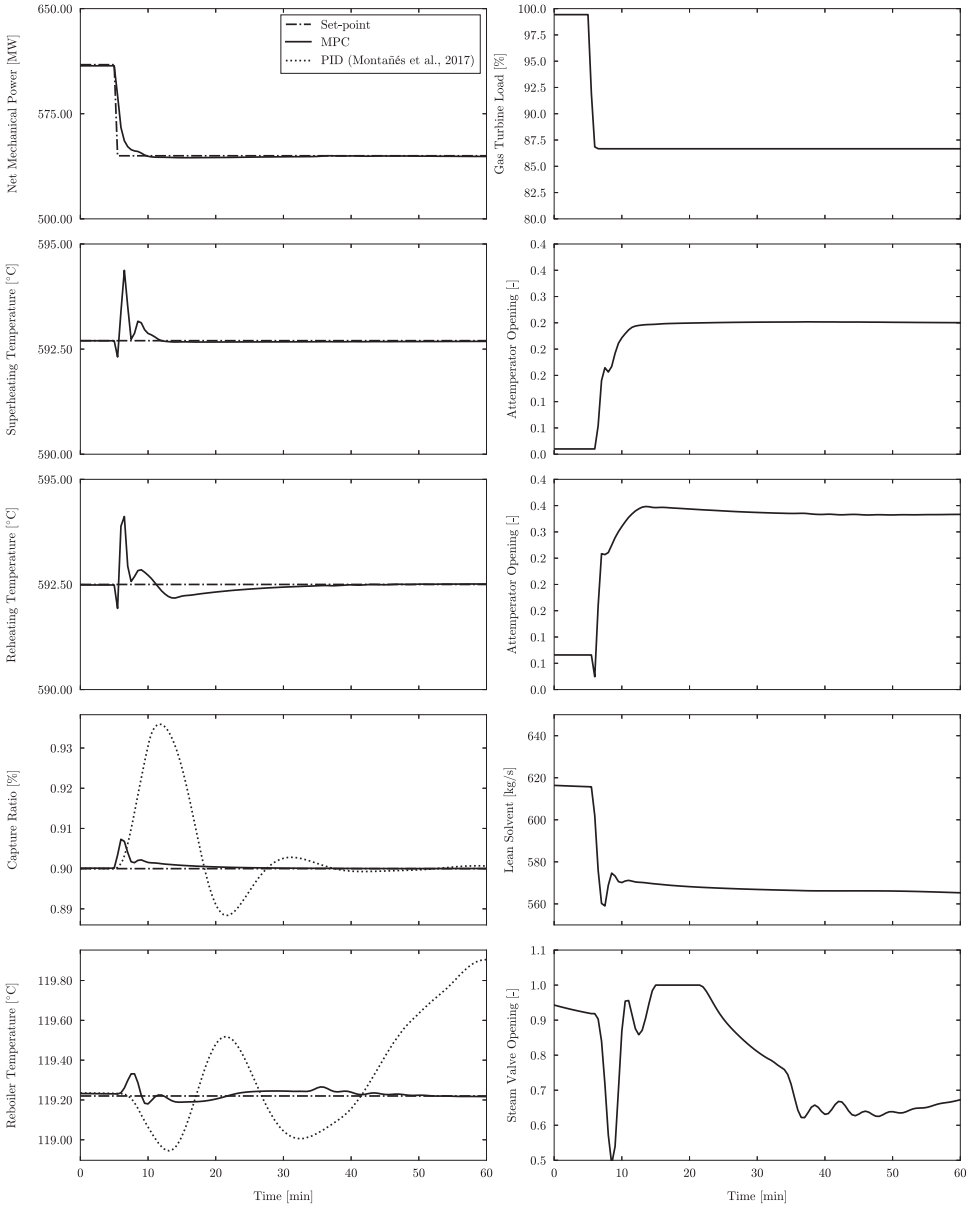

Fig. 3. Dynamic behaviour of process variables from the NGCC-PCC system with the proposed MPC strategy during a power demand reduction of 70 MW.

lustrates how traditional PID controllers require more time and lead to larger offsets than MPC, albeit offset-free control is also achieved because of their integral action (Montañés et al., 2017c).

In contrast, the reboiler temperature needed more time to reach its set-point. Control actions in the mass flow rate of lean solvent to stabilise the capture ratio modify the operation of the desorber, which also affects the lean loading of the solvent at the outlet of this column and the temperature in the reboiler. These process changes are characterised by slow dynamics because of the interaction between the absorber and stripper columns, large volumes of solvent and delays from piping and heat exchangers (Rúa et al., 2020b). Therefore, the MPC needs to adapt the steam extraction from the NGCC to anticipate the interaction between both absorption and desorption sections and compensate these operation changes. This leads to the saturation of the steam extraction valve in the first 20 min of transient performance of the CO_2 capture plant, which results from the combined effect of changing loading in the solvent, the MPC strategy trying to anticipate the dynamic behaviour of the reboiler temperature and the slow dynamics of the desorption section of the PCC plant. The steam cycle and capture stabilise completely during this time and reduce hence the variations in steam availability and fluctuation in the rich loading of the solvent. These steadier conditions ease the control of the reboiler temperature and allow a more stable and prolonged movements of the steam extraction valve after this stabilisation period.

Despite the saturation of the steam extraction valve, the proposed MPC strategy obtained smaller offsets than 0.15°C and achieved offset free in an hour, which is better performance than using PID controllers (Montañés et al., 2017c). This reduced offset achieved by the MPC strategy during drastic changes of load is specially important in the reboiler temperature, as it could allow increasing its set-point, and hence the stripping efficiency, without reaching temperatures that lead to solvent degradation during the regeneration process.

Tuning of the MPC was not the main objective of this study. Improved performance might be achieved with adequate weight values in the objective function, λ_Q and λ_R, disturbance matrices and vectors (Pannocchia, 2003), B_d and C_d, and noise models for

the Kalman estimator, Q_p and R_m. However, the different orders of magnitude among controlled and manipulated variables suppose a challenge to balance the values of these different tuning parameters.

5. Conclusions

Flexible thermal power plants integrated with post-combustion capture systems will play a fundamental role balancing the intermittent power generation from renewable energy sources with low-carbon electricity. The deployment of this technology requires, however, the demonstration that this type of power systems can provide fast changes of power output whilst capturing most of the produced CO_2. Optimisation-based control strategies can enhance the dynamic operation of these integrated systems and contribute to more efficient and stable power systems. Among the different available technologies to produce flexible, low-carbon power, natural gas combined cycles offer the fastest and most efficient performance.

This work presents a linear model predictive control strategy applied to a modern NGCC integrated with a PCC plant. This method achieves offset-free control by augmenting the linear model with a disturbance model that removes any deviation from the set-point. Furthermore, the proposed MPC strategy is formulated in delta-input form, since this form is easier to implement and more computationally efficient due to the reduced amount of optimisation variables. Linear, data-based models were developed and implemented in the MPC strategy because of the excessive computational cost of the high-fidelity dynamic models. System identification allowed the development of several data-based, local ARX models that were combined in a local model network capable of predicting nonlinear behaviour with a set of linear models. This approach permitted the formulation of the dynamic optimisation program in the MPC strategy as a convex quadratic programming (QP) problem that leads to global optimal solutions.

A case study where a NGCC integrated with a PCC plant needs to balance a step change in power demand demonstrated the effectiveness of the proposed MPC strategy. The key process variables controlled by the MPC presented offset-free in shorter periods of time than those observed with traditional PID controllers. Moreover, the deviations from the set-point during transient operation were smaller. This dynamic behaviour with reduced offsets allows the approximation of nominal values of these parameters to their limits, which could potentially lead to improved performance, e.g. reboiler temperature closer to the degradation limit of the solvent. Linear MPC also presents fast convergence time because of its convexity and favourable numerical properties. Thus, better dynamic operation could be achieved by reducing the sampling time and increasing the predicting horizon. Adequate selection of weights in the objective function, disturbance matrices and vectors, and noise models in the estimator could also lead to improvements in the dynamic performance of the NGCC-PCC system. This topic was not analysed in this study, but it is considered as an interesting direction for future research.

Declaration of Competing Interest

The authors declare that they have no known competing financial interests or personal relationships that could have appeared to influence the work reported in this paper.

Appendix A

Table A.4 summarises the coefficients of the local ARX models identified in Section 2.2. The combination of these parameters with a Gaussian validity function leads to the overall parameters that compose the local model network at each sampling time.

Table A.4
Coefficients of the simplified local ARX models composing the local model networks.

Controlled variable	γ	Local model	Centre	Parameters	
				a	b
Net power generation	-	-	-	90	5.25
Supeheated steam temperature	Gas turbine load	1	100	-1.21, 0.21	-23.06, 23.15
		2	95	-1.50, 0.50	-21.34, 21.46
		3	90	-1.29, 0.29	-24.03, 24.00
		4	85	-1.32, 0.32	-22.74, 22.90
		5	80	-1.34, 0.34	-22.22, 22.34
Reheated steam temperature	Gas turbine load	1	100	-1.06, 0.06	-14.58, 15.02
		2	95	-1.20, 0.20	-15.96, 16.09
		3	90	-1.17, 0.17	-15.10, 15.53
		4	85	-1.19, 0.19	-14.40, 15.08
		5	80	-1.21, 0.21	-14.37, 15.04
Capture ratio	Mass flow exhaust gas	1	436.5	-0.931	7.925e-5
		2	429	-0.938	7.543e-5
		3	412	-0.949	6.093e-5
		4	395	-0.978	2.156e-5
		5	379	-0.972	3.073e-5
Reboiler steam temperature	Mass flow exhaust gas	1	436.5	-0.992	0.166
		2	429	-0.981	0.225
		3	412	-0.997	0.219
		4	395	-0.993	0.089
		5	379	-0.996	0.110

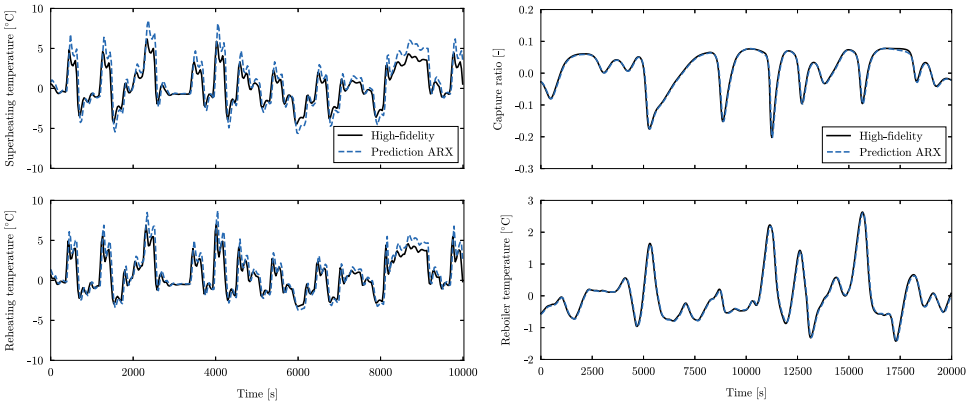

(a) Validation of the NGCC simplified models.

(b) Validation of the PCC simplified models.

Fig. B.4. Validation results of the simplified models described in Section 2.2. These results only include a small set of the validation data to ease the visibility, whereas the R^2 values on Table 1 considered the entire set.

Appendix B

Fig. B.4 illustrates a small set of the validation results comparing the predicting capability of the LMN of simplified ARX models and the output of the dynamic high-fidelity model.

Appendix C

Consider the control input action defined in Eq. (9) and substitute it in the simplified polynomial model in Eq. (4):

$$y_k = a + b\,(\delta u_k + u_{k-1}) \tag{C.1}$$

If the same sequences of outputs and control inputs over a time horizon N as in Section 3.1 are considered, this polynomial model can be expressed:

$$y = a\,I + b\,\Psi\,\delta u + b\,I\,u_{-1} \tag{C.2}$$

where I is the identity matrix and Ψ was defined in Section 3.1. Inserting this vector equation and the delta-input definition on the inequality constraints of the standard MPC formulation:

$$g_{\text{pow}}\,\delta u \le f_{\text{pow}} \tag{C.3}$$

where

$$g_{\text{pow}} = \begin{bmatrix} -b\Psi \\ b\Psi \\ -\Psi \\ \Psi \\ -I \\ I \end{bmatrix} \quad f_{\text{pow}} = \begin{bmatrix} -(y^{\text{low}} - aI - bIu_{k-1}) \\ y^{\text{up}} - aI - bIu_{k-1} \\ -(u^{\text{low}} - u_{k-1}) \\ u^{\text{up}} - u_{k-1} \\ \text{GT}_{\text{ramp}} \\ \text{GT}_{\text{ramp}} \end{bmatrix}$$

and GT_{ramp} limits the maximum ramping rate of the gas turbine. This work considers a 15%/min ramp rate, as indicated by most gas turbine manufacturers.

Similarly, the objective function becomes:

$$\begin{aligned} J_{\text{pow}} &= \frac{1}{2}\left(\|Q(y - y_{\text{ref}})\| + \|R\delta u\|\right) \\ &= \frac{1}{2}\left(\|Q(aI + b\Psi\delta u + bIu_{-1} - y_{\text{ref}})\| + \|R\delta u\|\right) \\ &= \frac{1}{2}\Big[\delta u^T (b^T\Psi^T Q\Psi b + R)\delta u \\ &\quad + 2(aI + bIu_{-1} - y_{\text{ref}})^T Q\Psi b\delta u \\ &\quad + (aI + bIu_{-1} - y_{\text{ref}})^T Q(aI + bIu_{-1} - y_{\text{ref}})\Big] \end{aligned} \tag{C.4}$$

These inequality constraints and objective function, Eqs. (C.3) and (C.4) respectively, define the MPC delta-input formulation in Eq. (14) for the polynomial model in Eq. (4). Thus, it may be easily combined with state-space models in the MIMO formulations described in Section 3.2.2.

CRediT authorship contribution statement

Jairo Rúa: Conceptualization, Methodology, Software, Validation, Formal analysis, Investigation, Visualization, Writing - original draft. **Magne Hillestad:** Writing - review & editing, Supervision. **Lars O. Nord:** Resources, Writing - review & editing, Supervision, Funding acquisition.

References

Alobaid, F., Mertens, N., Starkloff, R., Lanz, T., Heinze, C., Epple, B., 2017. Progress in dynamic simulation of thermal power plants. Progress in Energy and Combustion Science 59, 79–162.
Alobaid, F., Postler, R., Ströhle, J., Epple, B., Kim, H.-G., 2008. Modeling and investigation start-up procedures of a combined cycle power plant. Applied Energy 85 (12), 1173–1189.
Arce, A., Mac Dowell, N., Shah, N., Vega, L., 2012. Flexible operation of solvent regeneration systems for CO_2 capture processes using advanced control techniques: Towards operational cost minimisation. International Journal of Greenhouse Gas Control 11, 236–250.
Aske, E.M.B., Skogestad, S., 2009. Consistent inventory control. Industrial & Engineering Chemistry Research 48 (24), 10892–10902.
Borrelli, F., Morari, M., 2007. Offset free model predictive control. In: 2007 46th IEEE Conference on Decision and Control. IEEE, pp. 1245–1250.
Bui, M., Adjiman, C.S., Bardow, A., Anthony, E.J., Boston, A., Brown, S., Fennell, P.S., Fuss, S., Galindo, A., Hackett, L.A., et al., 2018. Carbon capture and storage (CCS): the way forward. Energy & Environmental Science 11 (5), 1062–1176.
Casella, F., Pretolani, F., 2006. Fast start-up of a combined-cycle power plant: a simulation study with modelica. In: Modelica Conference, 4, pp. 3–10.
Chen, B., 2013. Linear Systems Theory and Design.
Dassault Systemes, 2016. https://www.3ds.com/products-services/catia/products/dymola/.
Decardi-Nelson, B., Liu, S., Liu, J., 2018. Improving flexibility and energy efficiency of post-combustion CO_2 capture plants using economic model predictive control. Processes 6 (9), 135.
Dutta, R., Nord, L.O., Bolland, O., 2017. Selection and design of post-combustion CO_2 capture process for 600 MW natural gas fueled thermal power plant based on operability. Energy 121, 643–656.
Eser, P., Chokani, N., Abhari, R., 2017. Operational and financial performance of fossil fuel power plants within a high renewable energy mix. Journal of the Global Power and Propulsion Society 1, 16–27.
Flø, N.E., Knuutila, H., Kvamsdal, H.M., Hillestad, M., 2015. Dynamic model validation of the post-combustion CO_2 absorption process. International Journal of Greenhouse Gas Control 41, 127–141.
Flø, N.E., Kvamsdal, H.M., Hillestad, M., 2016. Dynamic simulation of post-combustion CO_2 capture for flexible operation of the brindisi pilot plant. International Journal of Greenhouse Gas Control 48, 204–215.
Forssell, U., Ljung, L., 1999. Closed-loop identification revisited. Automatica 35 (7), 1215–1241.
Garðarsdóttir, S.Ó., Montañés, R.M., Normann, F., Nord, L.O., Johnsson, F., 2017. Effects of CO_2-absorption control strategies on the dynamic performance of a supercritical pulverized-coal-fired power plant. Industrial & Engineering Chemistry Research 56 (15), 4415–4430.

Garðarsdóttir, S.Ó., Normann, F., Andersson, K., Prölß, K., Emilsdóttir, S., Johnsson, F., 2015. Post-combustion CO_2 capture applied to a state-of-the-art coal–fired power plant the influence of dynamic process conditions. International Journal of Greenhouse Gas Control 33, 51–62.
Gaspar, J., Ricardez-Sandoval, L., Jørgensen, J.B., Fosbøl, P.L., 2016. Controllability and flexibility analysis of CO_2 post-combustion capture using piperazine and mea. International Journal of Greenhouse Gas Control 51, 276–289.
Gevers, M., 2005. Identification for control: From the early achievements to the revival of experiment design. European journal of control 11, 1–18.
Gevers, M., Ljung, L., 1986. Optimal experiment designs with respect to the intended model application. Automatica 22 (5), 543–554.
Gevers, M., Mišković, L., Bonvin, D., Karimi, A., 2006. Identification of multi-input systems: variance analysis and input design issues. Automatica 42 (4), 559–572.
González-Salazar, M.A., Kirsten, T., Prchlik, L., 2017. Review of the operational flexibility and emissions of gas-and coal-fired power plants in a future with growing renewables. Renewable and Sustainable Energy Reviews 82, 1497–1513.
Hauger, S.O., Flø, N.E., Kvamsdal, H., Gjertsen, F., Mejdell, T., Hillestad, M., 2019. Demonstration of non-linear model predictive control of post-combustion CO_2 capture processes. Computers & Chemical Engineering 123, 184–195.
He, X., Wang, Y., Bhattacharyya, D., Lima, F.V., Turton, R., 2018. Dynamic modeling and advanced control of post-combustion CO_2 capture plants. Chemical Engineering Research and Design 131, 430–439.
He, Z., Sahraei, M.H., Ricardez-Sandoval, L.A., 2016. Flexible operation and simultaneous scheduling and control of a CO_2 capture plant using model predictive control. International Journal of Greenhouse Gas Control 48, 300–311.
Hentschel, J., Spliethoff, H., et al., 2016. A parametric approach for the valuation of power plant flexibility options. Energy Reports 2, 40–47.
Heuberger, C.F., Rubin, E.S., Staffell, I., Shah, N., Mac Dowell, N., 2017. Power capacity expansion planning considering endogenous technology cost learning. Applied Energy 204, 831–845.
Heuberger, C.F., Staffell, I., Shah, N., Mac Dowell, N., 2016. Quantifying the value of CCS for the future electricity system. Energy & Environmental Science 9 (8), 2497–2510.
Heuberger, C.F., Staffell, I., Shah, N., Mac Dowell, N., 2017. A systems approach to quantifying the value of power generation and energy storage technologies in future electricity networks. Computers & Chemical Engineering 107, 247–256.
Huusom, J.K., Poulsen, N.K., Jørgensen, S.B., Jørgensen, J.B., 2010. Tuning of methods for offset free mpc based on arx model representations. In: Proceedings of the 2010 American Control Conference. IEEE, pp. 2355–2360.
IEA, 2019. World Energy Outlook 2019. https://www.iea.org/reports/world-energy-outlook-2019.
IPCC, 2005. IPCC Special Report on Carbon Dioxide Capture and Storage. Prepared by Working Group III of the Intergovernmental Panel on Climate Change [Metz, B., O. Davidson, H. C. de Coninck, M. Loos, and L. A. Meyer (eds.)]. Cambridge University Press, Cambridge, United Kingdom and New York, NY, USA.
IPCC, 2014. Climate Change 2014: Synthesis Report. Contribution of Working Groups I, II and III to the Fifth Assessment Report of the Intergovernmental Panel on Climate Change [Core Writing Team, R.K. Pachauri and L.A. Meyer (eds.)], IPCC, Geneva, Switzerland.
IPCC, 2018. Summary for Policymakers. In: Global warming of 1.5°C. An IPCC Special Report on the impacts of global warming of 1.5°C above pre-industrial levels and related global greenhouse gas emission pathways, in the context of strengthening the global response to the threat of climate change, sustainable development, and efforts to eradicate poverty. [V. Masson-Delmotte, P. Zhai, H. O. Prtner, D. Roberts, J. Skea, P. R. Shukla, A. Pirani, W. Moufouma-Okia, C. Pan, R. Pidcock, S. Connors, J. B. R. Matthews, Y. Chen, X. Zhou, M. I. Gomis, E. Lonnoy, T. Maycock, M. Tignor, T. Waterfield (eds.)]. World Meteorological Organization, Geneva, Switzerland.
Johansen, T.A., Foss, B., 1993. Constructing NARMAX models using ARMAX models. International Journal of Control 58 (5), 1125–1153.
Jonshagen, K., Genrup, M., 2010. Improved load control for a steam cycle combined heat and power plant. Energy 35 (4), 1694–1700.
Jordal, K., Ystad, P.A.M., Anantharaman, R., Chikukwa, A., Bolland, O., 2012. Design–point and part-load considerations for natural gas combined cycle plants with post combustion capture. International Journal of Greenhouse Gas Control 11, 271–282.
Jung, H., Im, D., Heo, S., Kim, B., Lee, J.H., 2020. Dynamic Analysis and Linear Model Predictive Control for Operational Flexibility of Post-Combustion CO_2 Capture Processes. Computers & Chemical Engineering 106968.
Kalman, R.E., 1960. A new approach to linear filtering and prediction problems. Journal of Basic Engineering 35–45.
Kehlhofer, R., Hannemann, F., Rukes, B., Stirnimann, F., 2009. Combined-Cycle Gas & Steam Turbine Power Plants. Pennwell Books.
Kondziella, H., Bruckner, T., 2016. Flexibility requirements of renewable energy based electricity systems–A review of research results and methodologies. Renewable and Sustainable Energy Reviews 53, 10–22.
Lawal, A., Wang, M., Stephenson, P., Koumpouras, G., Yeung, H., 2010. Dynamic modelling and analysis of post-combustion CO_2 chemical absorption process for coal-fired power plants. Fuel 89 (10), 2791–2801.
Lawal, A., Wang, M., Stephenson, P., Obi, O., 2012. Demonstrating full-scale post–combustion CO_2 capture for coal-fired power plants through dynamic modelling and simulation. Fuel 101, 115–128.
Li, Z., Ding, Z., Wang, M., Oko, E., 2018. Model-free adaptive control for mea-based post-combustion carbon capture processes. Fuel 224, 637–643.
Ljung, L., 1987. System identification: theory for the user. Prentice-hall.
Lu, S., Hogg, B., 1997. Predictive co-ordinated control for power-plant steam pressure and power output. Control Engineering Practice 5 (1), 79–84.
Luu, M.T., Manaf, N.A., Abbas, A., 2015. Dynamic modelling and control strategies for flexible operation of amine-based post-combustion CO_2 capture systems. International Journal of Greenhouse Gas Control 39, 377–389.
Manaf, N.A., Cousins, A., Feron, P., Abbas, A., 2016. Dynamic modelling, identification and preliminary control analysis of an amine-based post-combustion CO_2 capture pilot plant. Journal of Cleaner Production 113, 635–653.
Mansour, F., Abdul Aziz, A., Abdel-Ghany, S., El-Shaer, H., 2003. Combined cycle dynamics. Proceedings of the Institution of Mechanical Engineers, Part A: Journal of Power and Energy 217 (3), 247–258.
Marx-Schubach, T., Schmitz, G., 2019. Modeling and simulation of the start-up process of coal fired power plants with post-combustion CO_2 capture. International Journal of Greenhouse Gas Control 87, 44–57.
Matsumura, S., Ogata, K., Fujii, S., Shioya, H., 1998. Adaptive control for the steam temperature of thermal power plants. In: Proceedings of the 1998 IEEE International Conference on Control Applications (Cat. No. 98CH36104), 2. IEEE, pp. 1105–1109.
Mechleri, E., Lawal, A., Ramos, A., Davison, J., Mac Dowell, N., 2017. Process control strategies for flexible operation of post-combustion CO_2 capture plants. International Journal of Greenhouse Gas Control 57, 14–25.
Mišković, L., Karimi, A., Bonvin, D., Gevers, M., 2008. Closed-loop identification of multivariable systems: With or without excitation of all references? Automatica 44 (8), 2048–2056.
Modelica Association, 2019. https://www.modelica.org/.
Modelon, 2015. Thermal Power Library. https://www.modelon.com/library/thermal-power-library/.
Montañés, R.M., Flø, N.E., Nord, L.O., 2017. Dynamic process model validation and control of the amine plant at CO_2 technology centre mongstad. Energies 10 (10), 1527.
Montañés, R.M., Flø, N.E., Nord, L.O., 2017. Dynamic process model validation and control of the amine plant at CO_2 Technology Centre Mongstad. Energies 10 (10), 1527.
Montañés, R.M., Flø, N.E., Nord, L.O., 2018. Experimental results of transient testing at the amine plant at technology centre mongstad: Open-loop responses and performance of decentralized control structures for load changes. International Journal of Greenhouse Gas Control 73, 42–59.
Montañés, R.M., Garðarsdóttir, S.Ó., Normann, F., Johnsson, F., Nord, L.O., 2017. Demonstrating load-change transient performance of a commercial-scale natural gas combined cycle power plant with post-combustion CO_2 capture. International Journal of Greenhouse Gas Control 63, 158–174.
Montañés, R.M., Korpås, M., Nord, L.O., Jaehnert, S., 2016. Identifying operational requirements for flexible CCS power plant in future energy systems. Energy Procedia 86, 22–31.
Nittaya, T., Douglas, P.L., Croiset, E., Ricardez-Sandoval, L.A., 2014. Dynamic modelling and control of mea absorption processes for CO_2 capture from power plants. Fuel 116, 672–691.
Panahi, M., Skogestad, S., 2011. Economically efficient operation of CO_2 capturing process part i: Self-optimizing procedure for selecting the best controlled variables. Chemical Engineering and Processing: Process Intensification 50 (3), 247–253.
Panahi, M., Skogestad, S., 2012. Economically efficient operation of CO_2 capturing process. part ii. design of control layer. Chemical Engineering and Processing: Process Intensification 52, 112–124.
Pannocchia, G., 2003. Robust disturbance modeling for model predictive control with application to multivariable ill-conditioned processes. Journal of Process Control 13 (8), 693–701.
Pannocchia, G., 2015. Offset-free tracking mpc: A tutorial review and comparison of different formulations. In: 2015 European control conference (ECC). IEEE, pp. 527–532.
Pannocchia, G., Rawlings, J.B., 2003. Disturbance models for offset-free model-predictive control. AIChE journal 49 (2), 426–437.
Peng, H., Wu, J., Inoussa, G., Deng, Q., Nakano, K., 2009. Nonlinear system modeling and predictive control using the rbf nets-based quasi-linear arx model. Control Engineering Practice 17 (1), 59–66.
Prasad, G., Irwin, G., Swidenbank, E., Hogg, B., 2000. Plant-wide predictive control for a thermal power plant based on a physical plant model. IEE Proceedings–Control Theory and Applications 147 (5), 523–537.
Prasad, G., Swidenbank, E., Hogg, B., 1998. A local model networks based multivariable long-range predictive control strategy for thermal power plants. Automatica 34 (10), 1185–1204.
Rawlings, J.B., Mayne, D.Q., Diehl, M., 2017. Model predictive control: theory, computation, and design, 2. Nob Hill Publishing Madison, WI.
Rezazadeh, F., Gale, W.F., Hughes, K.J., Pourkashanian, M., 2015. Performance viability of a natural gas fired combined cycle power plant integrated with post-combustion CO_2 capture at part-load and temporary non-capture operations. International Journal of Greenhouse Gas Control 39, 397–406.
Rúa, J., Agromayor, R., Hillestad, M., Nord, L.O., 2020a. Optimal dynamic operation of natural gas combined cycles accounting for stresses in thick-walled components. Appl. Ther. Eng. 114858.
Rúa, J., Bui, M., Nord, L.O., Mac Dowell, N., 2020b. Does CCS reduce power generation flexibility? A dynamic study of combined cycles with post-combustion CO_2 capture. International Journal of Greenhouse Gas Control 95, 102984.
Rúa, J., Nord, L.O., 2020. Optimal control of flexible natural gas combined cycles with stress monitoring: Linear vs nonlinear model predictive control. Appl. Energy 265, 114820. doi:10.1016/j.apenergy.2020.114820.

Sahraei, M.H., Ricardez-Sandoval, L., 2014. Controllability and optimal scheduling of a CO_2 capture plant using model predictive control. International Journal of Greenhouse Gas Control 30, 58–71.
Salvinder, K., Zabiri, H., Taqvi, S.A., Ramasamy, M., Isa, F., Rozali, N., Suleman, H., Maulud, A., Shariff, A., 2019. An overview on control strategies for CO_2 capture using absorption/stripping system. Chemical Engineering Research and Design 147, 319–337.
Schach, M.-O., Schneider, R., Schramm, H., Repke, J.-U., 2013. Control structure design for CO_2-absorption processes with large operating ranges. Energy Technology 1 (4), 233–244.
Thermoflow, 2014. GT Pro 24.0. Thermoflow Inc.
Walters, M.S., Edgar, T.F., Rochelle, G.T., 2016. Regulatory control of amine scrubbing for CO_2 capture from power plants. Industrial & Engineering Chemistry Research 55 (16), 4646–4657.
Wu, X., Shen, J., Li, Y., Wang, M., Lawal, A., Lee, K.Y., 2018. Nonlinear dynamic analysis and control design of a solvent-based post-combustion CO_2 capture process. Computers & Chemical Engineering 115, 397–406.
Wu, X., Shen, J., Li, Y., Wang, M., Lawal, A., Lee, K.Y., 2018. Nonlinear dynamic analysis and control design of a solvent-based post-combustion CO_2 capture process. Computers & Chemical Engineering 115, 397–406.
Wu, X., Shen, J., Li, Y., Wang, M., Lawal, A., Lee, K.Y., 2019. Dynamic behavior investigations and disturbance rejection predictive control of solvent-based post-combustion CO_2 capture process. Fuel 242, 624–637.
Wu, X., Wang, M., Liao, P., Shen, J., Li, Y., 2020. Solvent-based post-combustion CO_2 capture for power plants: A critical review and perspective on dynamic modelling, system identification, process control and flexible operation. Applied Energy 257, 113941.
Wu, X., Wang, M., Shen, J., Li, Y., Lawal, A., Lee, K.Y., 2019. Flexible operation of coal fired power plant integrated with post combustion CO_2 capture using model predictive control. International Journal of Greenhouse Gas Control 82, 138–151.
Wu, X., Wang, M., Shen, J., Li, Y., Lawal, A., Lee, K.Y., 2019. Reinforced coordinated control of coal-fired power plant retrofitted with solvent based CO_2 capture using model predictive controls. Applied Energy 238, 495–515.
Zhang, Q., Turton, R., Bhattacharyya, D., 2016. Development of model and model-predictive control of an mea-based postcombustion CO_2 capture process. Industrial & Engineering Chemistry Research 55 (5), 1292–1308.